Acta Polytechnica **65**(2):177–187, 2025
https://doi.org/10.14311/AP.2025.65.0177

Published by the Czech Technical University in Prague

PHOTOGRAMMETRIC IMAGE PROCESSING AND COMPARISON OF EXPERIMENTAL RESULT WITH LASER DIFFRACTION AND THE PDA METHOD

Adam Huněk*, Ondřej Bartoš

Czech Technical University in Prague, Faculty of mechanical engineering, Department of Energy engineering, Technická 4, 166 07 Prague, Czech Republic

* corresponding author: adam.hunek@fs.cvut.cz

Abstract. Optical methods have been established as a standard tool for aerosol size measurement. The aim of this paper is to compare the results of two commercial optical instruments based on Phase Doppler Anemometry (PDA) and Laser Diffraction (LD) with an in-house optical photogrammetric measurement method. For the purpose of this comparison, a new in-house image processing procedure was developed with the use of a MATLAB script. The accuracy of the method was tested on several calibration particle samples as well as on PDA and LD commercial instruments. The analysis of the measurements with calibration standard particles was done using the Bias-Variance decomposition method. All three methods were tested on the polydisperse sand particle sample. The results are applicable to determine the benefits and drawbacks of these methods in their application to the broader field of aerosol technology.

Keywords: Light scattering, phase Doppler anemometry, photogrammetry, image analysis, Otsu method, automatic thresholding.

1. Introduction

For the evaluation of the size distribution of polydisperse particle systems, certain optical methods have been established as standard diagnostic tools. In many cases of measuring the droplet size, these methods remain the only feasible means [1]. The motivation for this study arose from the analysis of liquid sprays and the study of liquid film breakup in steam turbines at transonic flow. In this scenario, droplets form on the trailing edge and are further accelerated to the bulk velocity of the steam flow. The accelerated droplets subsequently hit the rotating blades, causing erosion. The entire process contains the liquid film breakup, formation of droplets, and final flow in the carrier gas; these phenomena can be observed using various optical methods. Photogrammetry (also known as the shadowgraph imaging technique) plays an important role in observing the liquid film breakup and droplet acceleration. Alongside photogrammetry, Phase Doppler Anemometry (PDA) and light diffraction methods are used to measure the final aerosol (wet steam) flow. Moreover, PDA can also be used to measure the velocity at specific positions [2]. Because photogrammetry is applied at the beginning of the droplet formation process (focused on the blade's trailing edge), and the other two optical methods are used when the droplet formation process is complete, it is useful to identify the overlap between these methods. The goal of this paper is to compare all three methods as applied to monodisperse particles of 10, 15, 20, 30, 40, and 80 µm. A new in-house image processing procedure was developed for droplet size evaluation using a photogrammetric method based on the image obtained with a rapid exposure time. The MATLAB development environment was used. For practical applications, a test measurement was performed with a two-phase water nozzle. This nozzle is used in the experiment, where the nozzle generates water droplets, which subsequently saturate the neighbouring air. To set the required condition of the mixture, an exact understanding of the distribution of water droplets from the nozzle is necessary [3]. These results may then be generalised for similar situations, ultimately determining the measurement limitations of all the methods used. For this paper, the experiment was conducted in ambient air and open environment.

A similar method for aerosol size evaluation using image analysis was developed by Kashdan et al. [4]. This method is based on the evaluation of the diameter of the object by segmenting it with a specified threshold. The experimental setup consisted of a 12-bit CCD camera (PCO Sensicam) with a microscopic optical lens, providing a resolution of 0.7 µm/pixel. Illumination was provided by an infrared diode laser beam, which was diverged at a maximal angle with two prisms, and subsequently diffused with an opal glass lens to ensure even illumination of the photo. This paper focusses primarily on calibrating the depth of field with a Patterson globe and then determining the acceptable depth of field, derived from the linear calibration of the uncertain "halo area". The sensitivity of threshold determination decreases with the diameter of the object. Moreover, as the sensitivity decreases, it is necessary to ensure a sufficient difference between the background and object intensities.

Subsequently, a measurement was performed on a nozzle, and the comparison with a PDA measurement showed good agreement.

Among the published papers, comparisons of image analysis with other optical methods are very rare. Sijs et al. [5] compared laser diffraction, phase Doppler anemometry, and image analysis for several nozzles with an expected droplet diameter range of 150 µm to more than 550 µm. They found that larger droplets cause greater deviations in the evaluation of these methods. However, all methods are reliable for droplets up to approximately 400 µm. The main disadvantages of each method were identified. While the laser diffraction method is straightforward, it can inaccurately evaluate the increased distribution of smaller droplets as a result of their lower velocity, which leads to an increase in their concentration within the measurement volume. This effect has to be taken into account and the measurement has to be performed in a sufficiently large volume to avoid small particles accumulating in the measuring laser beam. Phase Doppler anemometry evaluation can be affected by air bubbles present in the droplets, which can then be falsely evaluated as smaller droplets. Herbst [6] compared the three optical methods for agricultural sprays, with droplet diameters ranging from approximately 100 to 500 µm, and found variations in the results of the individual methods that increased with larger droplet sizes. De Cock et al. [7] developed a high-speed imaging method and compared it with phase Doppler anemometry in ISO reference nozzles with droplet diameters ranging from 40 to 1 300 µm. The results, again, demonstrated comparable conclusions for smaller droplets, along with variations for larger ones. The imaging method tended to measure a similar Dv_{50}, a larger Dv_{90}, and a smaller Dv_{10} compared to the PDA. Kashdan et al. [8] developed a digital image analysis technique and compared it to PDA on a pressure-swirl atomiser for fuel droplets with diameters of 5 to 30 µm, finding slight differences in D_{10} (5 %) and D_{30} (3 %). The digital image analysis technique was able to detect large, non-spherical droplets that the PDA device could not detect. Kashdan et al. [9] then used the digital image analysis technique in a high-speed two-phase flow, using a pulsed laser for particle illumination with diameters ranging from 10 to 30 µm and velocities of up to 50 m s^{-1}, and compared it with PDA measurements. Both methods were highly compatible for objects larger than 25 µm. In recent years, comparisons of PDA and high-speed camera measurements of droplets from a water nozzle have been published, showing good agreement between the two methods [2].

Most of these published papers focus on distributions with droplets greater than 100 µm or those larger than 400 µm, which are often used in agriculture. The aim of this paper is to use samples with known monodisperse size distributions to calibrate the developed photogrammetric method and compare it to those of PDA (Dantec Dynamics) and Spraytec (Malvern Panalytical Ltd.). Subsequently, all of these methods are compared using non-monodisperse distributions for samples with particles ranging from 10 to 150 µm and a two-phase nozzle. This article is the culmination of a long-term research at the Department of Energy Engineering at CTU Prague on the identification of polydisperse systems. Partial results were recently published, for example, by Hunek [10]. The presented article also provides a complete set of experimental data and their processing.

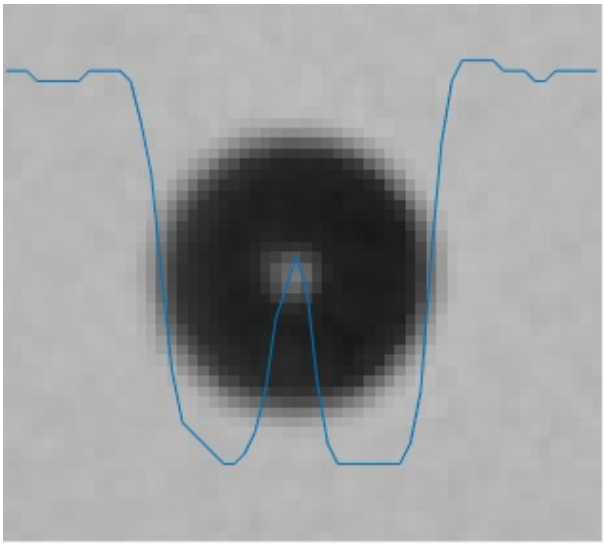

Figure 1. The detected object with the intensity values of the pixels at its axis.

2. The principle of image analysis methods for aerosol size measurement

Most image analysis methods for aerosol size measurement rely on capturing images with a short exposure time and a quick flash, typically in the order of microseconds, from a diode or laser, to capture rapidly moving objects. In the resulting greyscale image, the intensity distribution function theoretically has two peaks, representing pixels that clearly belong to the background and the object groups. However, there are many "uncertain" pixels that cannot be clearly determined. The main challenge of image analysis methods is to automatically determine whether these pixels are part of the object or background groups. An example of a detected aerosol is shown in Figure 1. The blue line represents the pixel intensity values along the horizontal axis of the aerosol. There is a well visible transition area between the object and the background (the "halo area") reported by Kashdan et al. [4], as well as light reflection at the centre of the aerosol. One possible method to segment these pixels is thresholding such as OTSU segmentation. To eliminate this uncertainty and achieve a reliable measurement method, a calibration is necessary.

2.1. OTSU SEGMENTATION

The photogrammetric method proposed in this paper is based on the OTSU segmentation of the object from the background, as proposed by Otsu [11]. This method can determine the threshold automatically and has the advantage of being fast and straightforward. The OTSU method uses a greyscale image histogram and attempts to find the borderline between the background and object pixels. The maximum value of between-class variance is used to get the optimal threshold k^* as described by the following equation:

$$\sigma_B^2(k^*) = \max_{1\le k<L} \sigma_B^2(k) = \max_{1\le k<L} \frac{[\mu_T \omega(k) - \mu(k)]^2}{\omega(k)[1-\omega(k)]}, \quad (1)$$

where

$[1,\ldots,k,\ldots,L]$ are the pixel levels,

$\omega(k) = \sum_{i=1}^{k} p_i$ is the zeroth-order cumulative moment of the histogram up to k pixel level,

$\mu(k) = \sum_{i=1}^{k} ip_i$ is the first-order cumulative moment of the histogram up to k pixel level,

$\mu_T = \sum_{i=1}^{L} ip_i$ is the overall mean,

p_i is the value of probability distribution at i^{th} pixel level [11].

Goh et al. [12] performed an analysis of the OTSU segmentation accuracy in the dependence of the object area to the segmentation area ratio, background intensity to the object intensity ratio, level of noise and position of the object. It was determined that the ideal object area to segmentation area ratio and ideal background intensity to object intensity ratio (for a dark object and light background) to avoid over-segmentation or under-segmentation is 72 % and 35 %, respectively. These ideal conditions apply to all levels of noise. As expected, the quality of segmentation is independent to the position of the segmented object.

3. OPTICAL METHODS

This chapter is devoted to a brief description of the two commercial optical devices, the PDA Dantec Dynamics and the Spraytec Malvern Panalytical. Subsequently, the developed photogrammetric method with the in-house MATLAB script is described.

3.1. THE PHASE-DOPPLER ANEMOMETER

The first optical device for the aerosol size measurement is the Phase-Doppler anemometer manufactured by Dantec Dynamics (Figure 2). The measurement setup consists of a laser with an adjustable power of up to 500 mW (continuous laser) and front lenses with a 350 mm focus length placed on the receiver. The detector is set in a forward refraction mode at an angle of 30° for all measurement cases. When measuring the duke standards, this configuration has the confidence of linearity of the PDA around 95.39 %. Although the optimal angle of the receiving optics for the case of water droplets in the air is approximately 68°, the confidence of linearity for the angle of 30° is 97.04 %, which is approximately 1 % less than the optimal angle. Depending on the expected aerosol size, the mask type A or B is used on the receiver. The light signal collected by the detection optics passes to a photomultiplier, activated by a voltage of 1 000 V. Compared to the laser diffraction method, the measurement volume is much lower, and the position of the device is controlled by a traversing system. The data are processed by flow control software, which is able to evaluate the diameter and velocity of each particle individually.

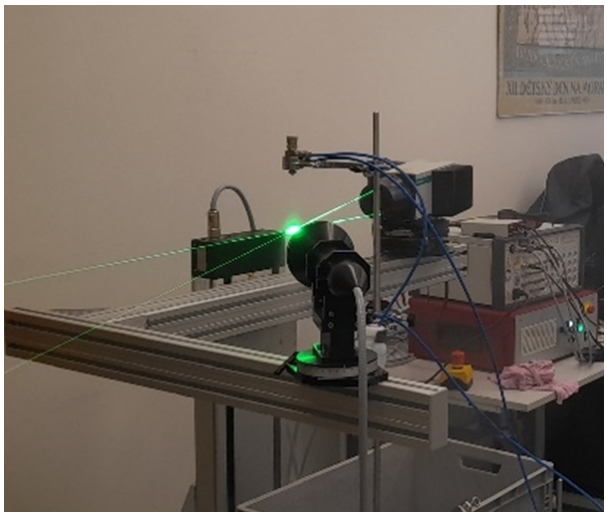

FIGURE 2. The Phase Doppler anemometer.

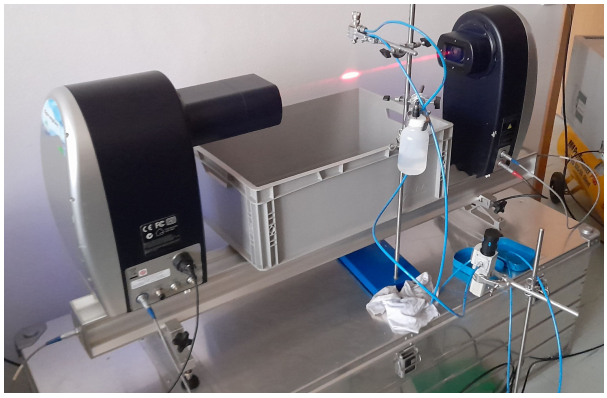

FIGURE 3. The Spraytec Malvern device.

3.2. LASER DIFFRACTION

The laser diffraction method is based on the Mie theory of angular light energy distribution of a scattered laser light at small angles. In this case, the commercial instrument, Spraytec Malvern, is used (Figure 3). It consists of a laser module with $\lambda = 635$ nm laser light and a receiver module with a 300 mm lens. The data from the receiver are continuously processed by a software that evaluates the particle size distribution. It can detect particles with diameters ranging from 0.1 µm to 1 mm.

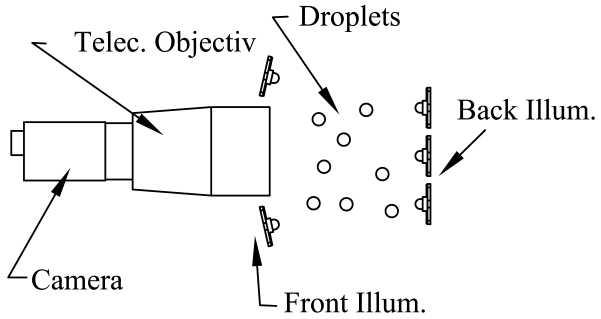

Figure 4. The typical Photogrammetry configuration.

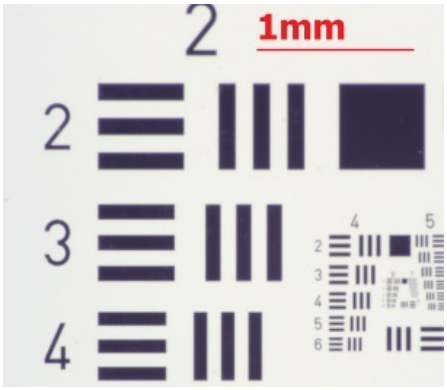

Figure 5. 1951 USAF resolution test chart.

3.3. The photogrammetric method (shadowgraph)

Similarly to the other image analysis methods for the evaluating droplet size, the photogrammetric method is based on taking pictures with a short exposure time and a quick flash from a diode in the order of microseconds to capture fast-moving objects. For this purpose, the XIMEA MC050CG-SY with Sony IMX250LQR-C digital sensor with $2\,464 \times 2\,056$ active pixels (3.4 µm pixel-pitch), and a telecentric lens was used. Sometimes the term "shadowgraph" is used. As shown in Figure 4, the flash is placed behind the spray cone so that the objects are represented by their shadow. For the calibration of the pixel-to-object size ratio, the 1951 USAF resolution test chart (Figure 5) was used. To evaluate object diameters from the images obtained, a new in-house MATLAB script was developed, the flowchart is shown on Figure 8. The aim of this method is to evaluate sharp objects, while eliminating those out of focus, which would not be evaluated accurately (Figures 6 and 7). The usage of a telecentric lens has the advantage of being independent of the detected object size to the distance of the object from the lens. However, this type of lens has a very narrow depth of field, which results in a blunter object concentration and many out-of-focus objects. This disadvantage can be eliminated by different approaches. First, the ratio between the out-of-focus distance and the gradient can be found [3] or, as was done for this paper, one can take more subsequent photos and only the focused objects are processed.

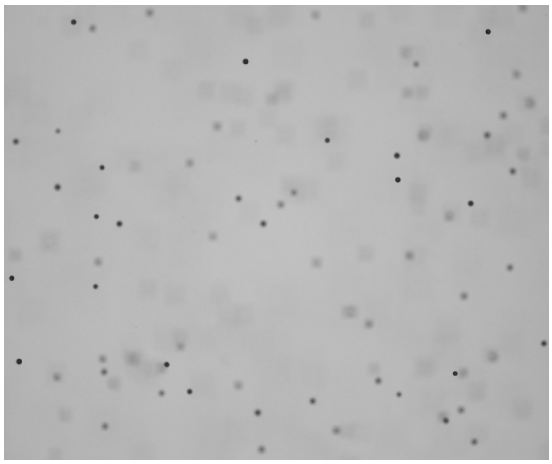

Figure 6. An example of a pre-processed image.

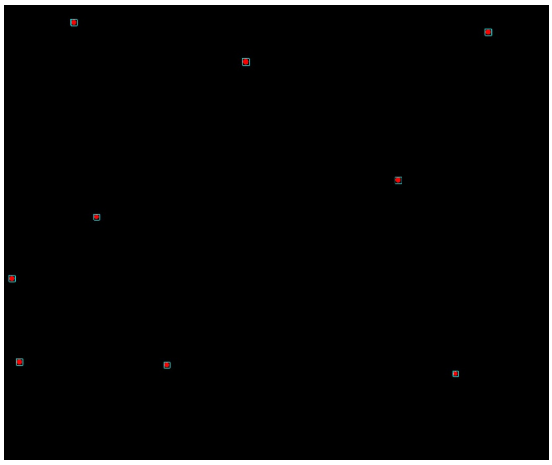

Figure 7. An example of a segmented image.

The OTSU threshold method was applied, as it possesses the advantage of quick evaluation and is able to automatically determine the threshold. First, the image is pre-processed to appropriately adjust it for the segmentation and to reduce the noise. Subsequently, the OTSU segmentation method is used throughout the picture to detect all objects. Then, the defocused objects are eliminated using the gradient method. This part of the script is applied for object detection and approximate object size evaluation in order to obtain an initial iteration of the ideal object-to-background ratio, which determines the required segmentation area for each detected object. The second part of the script is a loop with the possibility of additional iterations of the segmentation area. The purpose is to accurately segment each detected object individually according to the iterated segmentation area and to subsequently acquire the correct size distribution.

There are several adjustable parameters which affect the quality of the segmentation, and therefore the accuracy of this method. The source of this uncertainty (other than resolution) are the "uncertain pixels" between the clear object and the background pixels. The segmentation area adjusts the ratio of

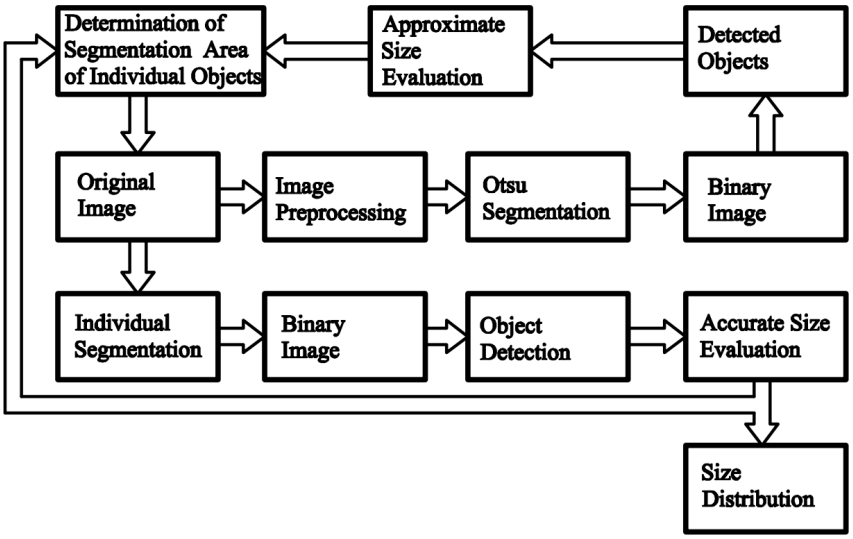

FIGURE 8. The photogrammetry image processing path.

the clear object and background pixels. In the script, it is adjusted with the parameter Segmentation window (dimensionless), which can be computed with the following Equation (2), where S_{object} represents the area of the detected object and $S_{\text{segmentation}}$ represents the area, around the object, where segmentation is performed, usually square or rectangle in shape.

$$\text{Segmentation window} = \frac{S_{\text{object}}}{S_{\text{segmentation}}}. \qquad (2)$$

The background intensity (contrast) changes the distance between the two peaks in the histogram of the picture. The gradient method eliminates objects according to the adjustable gradient boundary. Lower values of the gradient boundary could lead to an incorrect segmentation of out-of-focus objects, while higher values could lead to the non-inclusion of acceptable objects. The Gradient boundary is adjusted with the Gradient function as shown in Equation (3), where I_B represents a bright pixel with the 95^{th} percentile of pixel intensity value, while I_D represents the 200^{th} darkest pixel.

$$\text{Gradient boundary} = \text{Gradient function}\,(I_B - I_D)\,. \qquad (3)$$

Another adjustable parameter is the number of additional iterations of the ideal segmentation area. A lower number of additional iterations can lead to inaccuracy due to a differing segmentation area.

4. Calibrating the photogrammetric method

For the calibration of the photogrammetric method, six samples with latex particles of known monodisperse distributions of 10, 15, 20, 30, 40 and 80 micrometres were used. These particles were placed in a cuvette filled with water and equipped with a stirrer as shown in Figure 9. Information on all samples is shown in Table 1.

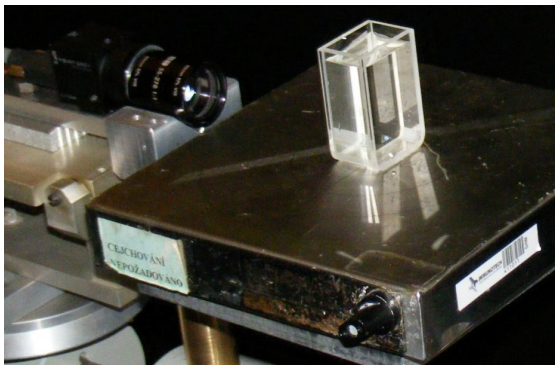

FIGURE 9. Photogrammetry measurement of a sample in cuvette.

Sample	1	2	3	4	5	6
D_{10} [µm]	10.1	14.97	20	30.07	39.6	81.4
s [µm]	0.9	0.13	0.2	0.3	3.6	1.5

TABLE 1. Information regarding all tested samples.

The photogrammetric measurement was performed by obtaining several pictures. In this case, the 8-bit monochromatic resolution was used. For each sample, three different intensity levels of the background pixels were taken. This corresponded to background intensity modes of 180, 150, and 110 on a scale from 0 to 255, where 255 represents the lightest intensity and 0 represents the darkest intensity. Here, the background intensity mode of 180 approximately corresponds to the ideal ratio of the object intensity to the background intensity as proposed by Goh et al. [12].

The evaluation of the in-house image processing method was done for several script configurations with variables of the segmentation window (Equation (2)) and the gradient function (Equation (3)). The number of additional iterations was set to 8, to minimise the iteration inaccuracy. The goal of the

calibration process was to find an ideal configuration of the evaluation of different particle sizes and different properties of the images. The individual output distributions were modified by the Grubbs test, which detected and erased outliers caused by impurities in the cuvette. Subsequently, the arithmetic mean and standard deviation were determined.

The measurement error was estimated using the theory of bias-variance decomposition [13]. This approach was chosen because the measurement error, determined in this way, includes all uncertainties in the measurement chain, the accuracy of the method, measurement facility, and systematic error of an experimenter. The authors performed all measurements with the utmost care to reduce these uncertainties. Firstly, the Bias (systematic error) of the measurement was computed by Equation (4), where D_{10m} is the arithmetic mean of the measurement and D_{10s} is the arithmetic mean of the sample.

$$\text{Bias} = D_{10m} - D_{10s}. \tag{4}$$

The random error is defined by Equation (5), where s_m is the standard deviation of the measurement and s_m^2 is the variance of the measurement. According to the law of total variance [14], the variance of the measurement contains the variance of the sample, the variance of the photogrammetric method, and noise. This means that the reference value of the error computation is the arithmetic mean of the sample.

$$\text{Random error} = s_m^2. \tag{5}$$

The Absolute error (AE) is then defined as the combination of the systematic and random errors, by the following:.

$$\text{AE} = \sqrt{\text{Bias}^2 + \text{Random error}}. \tag{6}$$

Finally, the Relative error (RE) is computed using Equation (7), where D_{10} is the mean of the sample:

$$\text{RE} = \frac{\text{AE}}{D_{10s}}. \tag{7}$$

Figure 10 shows the evaluation of sample 5 ($D_{10} = 39.6\,\mu\text{m}$), where the dependence of the relative error on the Segmentation window and the Gradient function is shown. In this case, the mode of the background pixel intensities was estimated to be 183. The figure shows a strong dependence of the Segmentation window on the Relative error (RE) with clear minimal values in each Gradient function level. RE also depends on the gradient function until approximately Gradient function = 0.6. This is the value where the out of focus objects are eliminated, and rising the value would lead to rejecting the objects that are focused. Setting the Gradient function to 0.6, the ideal value of the Segmentation window was estimated to be 0.64, slightly deviating from the value of 0.72 reported in [12]. Similarly, Figure 11 shows

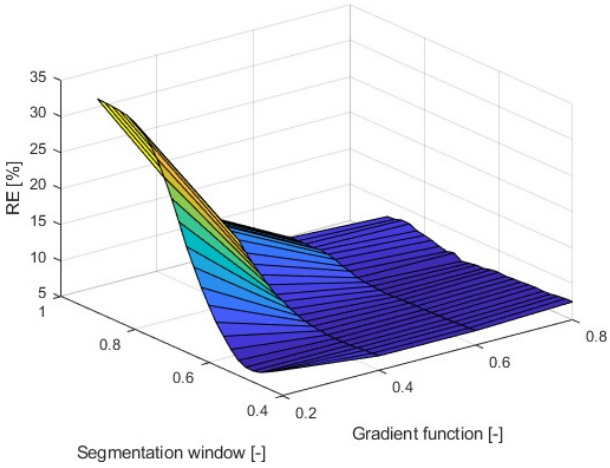

Figure 10. The calibration of the photogrammetry method – sample 5 ($D_{10} = 39.6\,\mu\text{m}$), where the dependence of the relative error on the Segmentation window and the Gradient function is shown. In this case, the mode of the background pixel intensities was estimated to be 183.

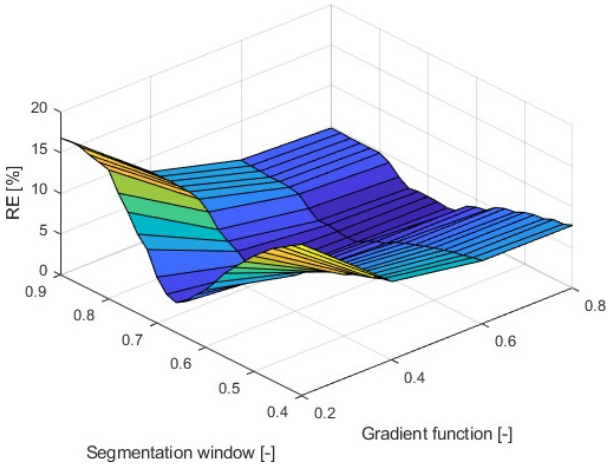

Figure 11. The calibration of the photogrammetry method – sample 3 ($D_{10} = 20\,\mu\text{m}$), where the mode of background pixel intensities is 184.

the evaluation of sample 3 ($D_{10} = 20\,\mu\text{m}$), where the mode of background pixel intensities is 184. The evaluation shows a similar trend, however, the ideal segmentation window for Gradient function = 0.6 is 0.68, which is closer to the value of 0.72 reported by Goh et al. [12].

Subsequently, the gradient function was set to 0.6 and the rest of the calibration was carried out. Table 2 shows the optimal segmentation window for the individual samples and background intensities along with the relative error (RE) and other evaluations. The results show dependence on the mode of the background intensity, as lower values (darker images) lead to under-segmentation. For darker images, the ideal segmentation window must be set higher. The results also show a strong dependence of the object size on the ideal segmentation window, as the evaluation of smaller objects requires the segmentation window to

Sample	Background intensity	Segmentation window	RE [%]
1	191	0.88	6.42
1	151	0.88	6.83
1	110	0.88	7.82
2	197	0.78	2.51
2	156	0.78	3.00
2	118	0.80	2.63
3	184	0.68	2.30
3	155	0.74	2.08
3	107	0.76	1.48
4	211	0.62	1.59
4	161	0.62	1.56
4	115	0.70	1.73
5	183	0.64	6.59
5	145	0.66	7.29
5	101	0.72	2.94
6	199	0.48	4.21
6	154	0.56	4.47
6	94	0.54	3.93

TABLE 2. The evaluation of the photogrammetry calibration.

be higher and, conversely, the evaluation of larger particles requires the segmentation window to be lower.

The charts in Figures 10 and 11, together with Table 2, show that the evaluation of the droplet size is dependent on the image properties. The optimal value of gradient function, segmentation window, and background intensity level are possible to find. This has to be taken into account for proper data processing.

5. The result of comparing the optical methods using monodisperse particle samples

A new set of photogrammetric measurements of the samples was carried out. The goal was to capture images with the optimal background intensities. The evaluation script was supplemented by the ideal values of the segmentation window for individual object sizes, and the gradient function was set to 0.6. In addition to the photogrammetric method, these samples were also evaluated by the Spraytec Malvern device based on laser diffraction and the Phase-Doppler anemometer by Dantec Dynamics (PDA). The goal was to verify the photogrammetric method and to compare these methods. Spraytec measurement was done continuously for 1 minute for each sample, and the PDA was set to a limit of 1 000 detected particles. The advantage of the Spraytec measurement was the possibility of calibration of the transmitted light previously to the addition of the samples, while the photogrammetry and PDA evaluation is affected by impurities in the cuvette. As the monodisperse samples are measured in the cuvette, the window correction in the PDA evaluation was used. Subsequently, the evaluation settings were carried out so that only high-quality signals were evaluated. For this purpose, a high signal-to-noise ratio of 5 dB and high 1st to 2nd peak ratio of 8:1 were set. Additionally, the phase validation ratio was set to 5 %. The centre and span of velocity were set to minimal values because of the slowly moving particles in the cuvette. The power of the laser was set to 31 mW, the sensitivity of the photomultipliers was set to 1 000 V, and the gain to 20 dB.

In the case of Photogrammetric and PDA evaluation, the Grubbs test was used to eliminate outliers caused by the impurities in the cuvette as described in the chapter of the photogrammetric calibration. To compare the evaluation of all samples with each of the individual methods, the volumetric size distribution and dimensionless diameter D_f was used. The dimensionless diameter D_f is defined by Equation (8), where d is the diameter corresponding to the Vof specific value of the function in the volumetric size distribution and D_{10s} is the arithmetic mean diameter of the corresponding sample.

$$D_f = \frac{d}{D_{10s}}. \tag{8}$$

By comparing the results with the theoretical distributions of the samples, the absolute and relative errors were estimated (Equations (6) and (7)). The resulting volumetric size distributions are shown in Figure 12. This figure mainly serves for verification of how much the mode and each evaluated distribution coincide with the theoretical arithmetic mean diameter D_{10}. All methods show very good accuracy for most samples. However, each method has certain disadvantages. The photogrammetry method has a mostly identical modification to the theoretical value, but is the most affected by the impurities in the cuvette. However, this disadvantage was eliminated by the Grubbs test. The Spraytec measurement is calibrated prior to the dosing of the standard duke samples dosing and is affected the least. The Spraytec measurement in Sample 6 has a correct mode; however, the distribution is wider. The PDA measurement seems to be less accurate for Samples 1 and 5, but the information on the velocity distribution of particles is available as well. All methods evaluated slightly smaller droplets during the measurements of Sample 4.

Table 3 shows the evaluation of all samples with the individual methods, where D_{10} is the arithmetic mean, s is the standard deviation, D_{32} is the Sauter mean diameter, AE is the absolute error, RE is the relative error, and N is the number of evaluated particles. The absolute error of the photogrammetry evaluation ranges from around 0.7 µm to 3.9 µm. This corresponds to the descending relative error from 8.13 % of Sample 2 to 3.64 % of Sample 6. Comparing these values to the evaluation of the other methods verify that the photogrammetric method is able to evaluate the monodisperse distributions comparably to the other two methods. The relative error of the Spraytec measurement ranges from 10.37 % to 5.78 % and the relative error of the PDA measurement ranges from

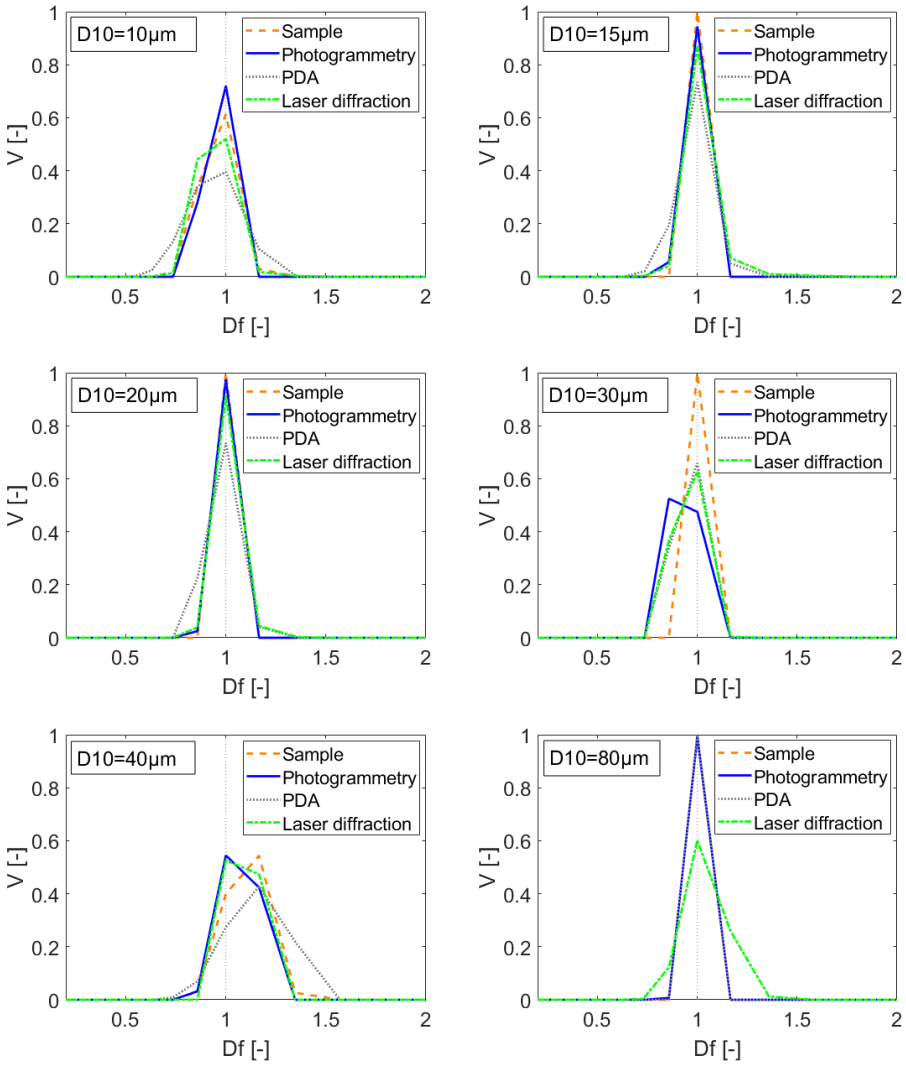

Figure 12. The volumetric size distributions of each sample.

17.04 % to 3.20 %. These results show that when the photogrammetry detects a particle (assuming thin spray), it is able to evaluate the size very accurately. The main obstacle for an accurate photogrammetric evaluation is the background intensity values and object sharpness, which are related to the exposure time and flash. In the case of dense spray measurement and the measurement of fast-moving objects with the exposure time set in order of μs, the resulting picture has a darker background. The results shown in Table 2 show very good agreement when measuring the same samples with a different exposure time and subsequently evaluating them with different Segmentation window values.

Comparing the evaluated photogrammetry measurement (Table 3) with the calibration shown in Table 2, the relative error is slightly higher. This might be caused by a slightly different reference sample or different settings for image acquisition. Although the goal was to acquire images with the mode of background pixel intensities around the value 180, it is tricky to adjust the settings. However, the relative error is still mostly less than 7 %, which is acceptable. The sample 5 has a wider standard deviation so even the results are affected by this fact and the deviation of the results is bigger than for other samples for all three methods. In all cases, the measurement was done with the same sample for all three methods to measure with the same cuvette and same concentration.

The aim of this measurement is not to denigrate any of the methods used, but to show their behaviour under the same conditions. For example, the PDA seems to be less accurate, but the mean diameters (D_{10}, D_{32}) are in good agreement with the original samples, only the final distribution is wider. This knowledge can be generalised, because all methods are very precise to determine the mean diameters (D_{10}, D_{32}), but the description of the distribution is usually wider. The explanation can come from the data processing of the raw optical signal. In this paper, we mention that the reason for the wider distribution for the photogrammetric method may be coagulated particles. Despite the effort to avoid the junction of two or more particles, some “doublets” can appear. The two tested commercial facilities are using the data processing without providing the necessary details.

	Sample	1	2	3	4	5	6
Duke standards	D_{10} [µm]	10.1	14.97	20	30.07	39.6	81.4
	s [µm]	0.9	0.13	0.2	0.3	3.6	1.5
Photogrammetry	D_{10} [µm]	10.13	14.15	19.19	29.17	38.30	79.64
	s [µm]	0.66	0.42	0.30	0.41	2.67	1.71
	D_{32} [µm]	10.22	14.18	19.20	29.18	38.68	79.71
	AE [µm]	0.70	0.94	0.96	1.09	3.22	3.91
	RE [%]	6.94	6.25	4.79	3.64	8.13	4.80
	N [#]	571	568	487	327	455	102
Laser diffraction	D_{10} [µm]	9.87	14.62	19.86	29.46	39.08	79.34
	s [µm]	0.88	1.47	1.15	2.74	2.95	8.18
	D_{32} [µm]	10.03	17.40	20.72	31.62	39.53	81.23
	AE [µm]	0.91	1.51	1.16	2.81	3.00	8.44
	RE [%]	9.03	10.09	5.78	9.35	7.58	10.37
PDA	D_{10} [µm]	9.35	14.00	19.25	29.58	39.55	80.74
	s [µm]	1.33	1.18	1.34	1.90	5.40	2.30
	D_{32} [µm]	9.72	14.19	19.43	29.83	40.99	80.87
	AE [µm]	1.72	1.98	1.71	2.29	6.14	2.60
	RE [%]	17.04	13.21	8.56	7.62	15.51	3.20
	N [#]	1 000	1 000	1 000	1 000	1 000	1 000

TABLE 3. The measurement evaluation.

Sample	Dv_{10} [µm]	Dv_{50} [µm]	Dv_{90} [µm]
7	36.56	60.59	88.36

TABLE 4. Information on Sample 7 as defined by its manufacturer.

6. The example of polydisperse distribution measurement

This chapter introduces an example of the measurement with all three methods. The measured sample contains sand particles ranging from 15 to 150 micrometres in length with the distribution shown Table 4. This sample was mixed in the water in the cuvette. The results are shown in Table 5 and Figure 13. To prevent sedimentation of the particles in the corners of the cuvette, it was mixed with a magnetic mixer. The phase Doppler anemometry is the most accurate according to Dv_{10} and photogrammetry, and Spraytec is the most accurate according to Dv_{50}. The Dv_{90} percentile is distorted by the impurities in the cuvette and by the clustering of the particles.

The analysis of the results has to include all the aspects of practical measurement. During the measurement, the homogeneity of the sample in the cuvette must be ensured by sample mixing, which helps to avoid the sedimentation of bigger particles. The unwanted presence of foreign particles would also affect the result. The optical measurement is also sensitive to sphericity of the particle, refraction index of particles, dispersant, and other parts of the optical measurement chain. The resulting difference between the declared diameter Dv_{50} of the polydisperse sample and the measured value is, for all measurements, lesser than 5 %. This photogrammetry measurement was performed according to the data processing mentioned above, as well as the PDA and light scattering measurement. The Sauer mean diameter is listed in Tab. 5 to compare the results with the same parameter as in previous cases. Unfortunately, the original polydisperse sample does not have D_{32} defined by the manufacturer and an assumption of normal distribution does not fit well.

7. Conclusion

The in-house photogrammetric method was tuned and compared with two optical methods, laser diffraction (Spraytec Malvern) and phase Doppler anemometry (PDA Dantec Dynamics), for aerosol size measurement. Six Duke samples with known, mostly monodisperse size distributions were dosed into a cuvette filled with filtered and demineralised water, and then evaluated by the three optical methods. The photogrammetric method was assessed for different background intensity levels to measure accurately for the non-optimal measurements of the wider range of real applications. The results showed that the accuracy of the developed photogrammetric method was comparable with other two optical methods. The results indicate that the measurements of the particles are in very good agreement for all three methods; the uncertainty of the measurements was determined. As an example of the practical measurement, all methods were compared using polydisperse distributions in a sample with known volumetric percentile diameters.

Sample	Dv_{10} [µm]	Dv_{50} [µm]	Dv_{90} [µm]	D_{32} [µm]
Photogrammetry	40.36	61.93	84.95	61.79
LD – Spraytec	40.05	61.15	89.08	60.98
PDA	37.26	57.44	86.35	56.77

Table 5. Information on Sample 7 as defined by its manufacturer.

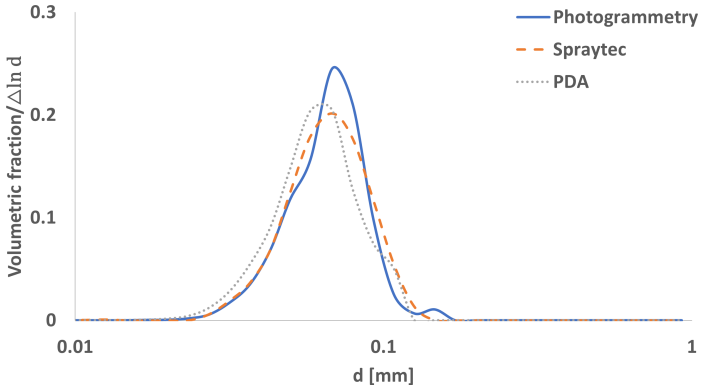

Figure 13. The volumetric size distributions of Sample 7.

Maximum effort was devoted to acquiring a clean sample, the photogrammetric and PDA evaluation samples may have been affected by impurities in the cuvette, while the Spraytec measurement was calibrated before the dosing of the samples. The effect of particle binding was suppressed by using a small amount of surfactant, but some clusters or impurities can appear. Generally, it can be supposed that the measurement with the monodispersed and polydisperse particles is sufficiently precise for all methods in the tested range of particles.

The purpose of this paper is not to make a competition between the optical methods, as all the methods tested are great and well established, and each of them has its advantages. However, there is an overlap between them. There are known examples in which two methods were used for the same measurement, but with slightly different results. This has led to unfair accusations against one of the methods. The purpose of this paper is to introduce the alternative approach for processing photogrammetric images and also to show their results obtained for the measurement, as similar as possible. The resulting accuracy, in the ideal case, shows that any of the methods has a significant advantage over the calibration measurement that was performed in this work.

All three methods are reliable and accurate, although it is necessary to understand the advantages and disadvantages of their data processing chains. Despite the simplicity of the advantage of the Spraytec device, it can be sensitive to parasitic light. The PDA device is a highly robust point measurement; however, it might be difficult to correctly setup. The developed photogrammetric method proved to be sufficiently accurate compared to the other two methods. The main limitations of this method include the pixel-to-object ratio, exposure time, flash duration, quality of the image, and the sphericity of the object. In addition, the method might not detect low numbers of density large particles that do, however, prove significant in regard to volumetric size distribution. Eliminating these disadvantages under certain conditions can result in a very reliable method for aerosol size measurement. The use of standard particles yields a valuable data set that is valuable to other users of each method.

List of symbols

D_{10} Mean diameter [µm]
D_{32} Sauter mean diameter [µm]
Dv_{10} Volumetric 10 percentile diameter [µm]
Dv_{50} Volumetric 50 percentile diameter [µm]
Dv_{90} Volumetric 90 percentile diameter [µm]
d Diameter corresponding to the value of distribution [mm]
D_f Volumetric size distribution dimensionless diameter [-]
s Standard deviation
V Volumetric or mass fraction (normalize) [Fraction/$\Delta \ln D_f$]

Acknowledgements

We gratefully acknowledge the support of the Grant Agency of the Czech Republic Grant No. 22-28869S.

References

[1] W. C. Hinds. *Aerosol technology: Properties, behaviour and measurement of airborne particles.* John Wiley, New York, USA, 1999.

[2] O. Cejpek, M. Malý, J. Jedelský. Combined drop sizing using phase Doppler anemometry and high-speed imaging. *AIP Conference Proceedings* **2672**(1):020001, 2023. https://doi.org/10.1063/5.0120006

[3] R. Xu, Z. Huang, W. Gong, et al. Depth from Defocus technique for irregular particle images. *Measurement* **238**:115156, 2024. https://doi.org/10.1016/j.measurement.2024.115156

[4] J. T. Kashdan, J. S. Shrimpton, A. Whybrew. Two-phase flow characterization by automated digital image analysis. Part 1: Fundamental principles and calibration of the technique. *Particle & Particle Systems Characterization* **20**(6):387–397, 2004. https://doi.org/10.1002/ppsc.200300897

[5] R. Sijs, S. Kooij, H. J. Holterman, et al. Drop size measurement techniques for sprays: Comparison of image analysis, phase Doppler particle analysis, and laser diffraction. *AIP Advances* **11**(1):015315, 2021. https://doi.org/10.1063/5.0018667

[6] A. Herbst. Droplet sizing on agricultural sprays – A comparison of measuring systems using a standard droplet size classification scheme. In *ILASS-Europe*, vol. 17, pp. 397–402. 2001.

[7] N. D. Cock, M. Massinon, D. Nuyttens, et al. Measurements of reference ISO nozzles by high-speed imaging. *Crop Protection* **89**:105–115, 2016. https://doi.org/10.1016/j.cropro.2016.07.016

[8] J. T. Kashdan, J. S. Shrimpton, A. Whybrew. Two-phase flow characterization by automated digital image analysis. Part 2: Application of PDIA for sizing sprays. *Particle and Particle Systems Characterization* **21**(1):15–23, 2004. https://doi.org/10.1002/ppsc.200400898

[9] J. T. Kashdan, J. S. Shrimpton, A. Whybrew. A digital image analysis technique for quantitative characterisation of high-speed sprays. *Optics and Lasers in Engineering* **45**(1):106–115, 2007. https://doi.org/10.1016/j.optlaseng.2006.03.006

[10] A. Huněk, O. Bartoš. The comparison of laser diffraction, PDA and photogrammetry for aerosol measurement. In *MATEC Web of Conferences*, vol. 383, p. 00011. 2023. https://doi.org/10.1051/matecconf/202338300011

[11] N. Otsu. A threshold selection method from gray-level histograms. *IEEE Transactions on Systems, Man and Cybernetics* **9**(1):62–66, 1979. https://doi.org/10.1109/TSMC.1979.4310076

[12] T. Y. Goh, S. N. Basah, H. Yazid, et al. Performance analysis of image thresholding: Otsu technique. *Measurement* **114**:298–307, 2018. https://doi.org/10.1016/j.measurement.2017.09.052

[13] J. Gao. Bias-variance decomposition of absolute errors for diagnosing regression models of continuous data. *Patterns* **2**(8):100309, 2021. https://doi.org/10.1016/j.patter.2021.100309

[14] J. K. Blitzstein, J. Hwang. *Introduction to probability*. Chapman and Hall / CRC Press, New York, USA, 2014. https://doi.org/10.1201/b17221